Preliminary Design of a TE Morphing Surface for Rotorcraft

Zahoor, Yasir; De Breuker, Roeland; Voskuijl, Mark

DOI
10.2514/6.2020-1301

Publication date
2020

Document Version
Final published version

Published in
AIAA Scitech 2020 Forum

AIAA SciTech Forum
6-10 January 2020, Orlando, FL
AIAA Scitech 2020 Forum

10.2514/6.2020-1301

Preliminary Design of a Trailing Edge Morphing Surface for Rotorcraft

Yasir Zahoor[1] and Roeland De Breuker[2]
Delft University of Technology, 2629 HS, The Netherlands

Mark Voskuijl[3]
Netherlands Defence Academy, 1780 AC, The Netherlands

This paper presents an overview of the preliminary design process and findings aimed at morphing of trailing edge (TE) control surfaces for rotorcraft. A design methodology for a camber morphing control surface is presented, although twist can also be induced by applying differential camber of the morphing section span. The concept investigated relies on utilizing conventional aircraft structures and materials for morphing purposes; thus, in essence, has the potential to fulfil the conflicting requirements of lightweight, flexibility and strength at the same time. Based on this concept, the preliminary design work shows that an active trailing edge camber morphing mechanism can be designed after careful considerations of design and actuation requirements. The numerical results presented also indicate that such a morphing scheme increases the 2D aerodynamic efficiency.

I. Nomenclature

μ	=	Advance ratio
α	=	Angle of attack, deg
c	=	Blade chord, mm
Cd	=	Drag coefficient
Cl	=	Lift coefficient
EI_{flap}	=	Effective flap bending rigidity, Nm^2
EI_{lag}	=	Effective lag bending rigidity, Nm^2
GJ	=	Effective GJ of cross section, Nm^2
M	=	Mach number
R	=	Rotor radius, m
ω	=	Rotor speed, rad/sec

II. Introduction

Morphing is a term that stems from the Greek word Metamorphosis and links to the processes involving shape change. Keeping the flying platform perspective, these shape changes are primarily associated with the wing of an aircraft or blade of a rotorcraft. This idea of "smooth" shape change arises from the much-needed requirement of drag reduction and improved flow quality. Therefore, a wing design with morphing capability can not only increase efficiency, maneuverability and performance but also can extend flight envelope of an aircraft. For helicopters, a blade with morphing capability can be utilized for primary control, performance gain or mitigating noise and vibration [1],[2], [3].

[1] PhD Researcher, Aerospace Structures and Computational Mechanics, Faculty of Aerospace Engineering, Kluyverweg 1; Delft, The Netherlands.
[2] Associate Professor, Aerospace Structures and Computational Mechanics, Faculty of Aerospace Engineering, Kluyverweg 1; Delft, The Netherlands, AIAA Senior member.
[3] Professor, Faculty of Military Sciences; Den Helder, The Netherlands, AIAA Member.

Implementation of a morphing concept is never straightforward, but when designing a morphing concept for helicopters, the challenges are often increased due to the complex loading environment and scarcity of internal blade volume, further limiting the choice of morphing solutions. Fig. 1 is a representation of the data presented by Barbarino et al. [4] for both fixed and rotary wing aircraft and is indicative of the fact that, although researchers have worked on numerous concepts, yet many of those did not make it to the prototype development and testing. This trend diminishes further for helicopters owing to the additional complexities involved as shown in Fig. 1.

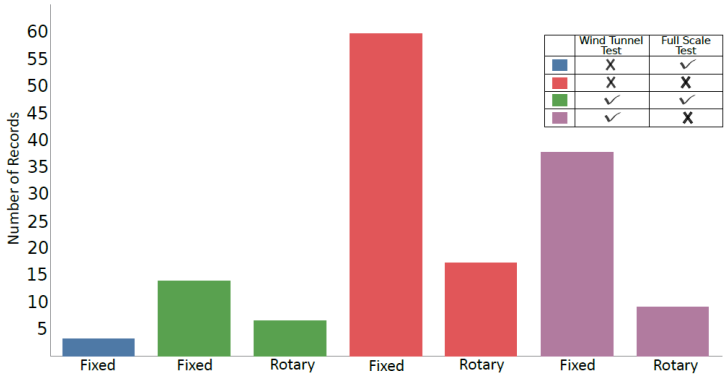

Fig. 1 Morphing concepts with respect to testing.

Morphing is considered a subjective term, and both the extent and the way of its implementation in a wing depends on the requirements specific to a particular type of aircraft. In case of helicopters, the additional complexity can be noticed in Fig. 2 where even in the case of hover, different blade sections encounter different flow velocities resulting in a linear variation of Mach number over the rotor radius (see Fig. 2a). In case of the forward flight, the aerodynamic environment becomes even more complicated and the Mach number at the blade sections also becomes a function of forward flight speed and blade azimuth position (see Fig. 2b). In addition, the flow velocities also depend on the inflow through the rotor disk and the flapping motion of the rotor blades in forward flight. Therefore, the angle of attack and associated blade loading is even more complicated.

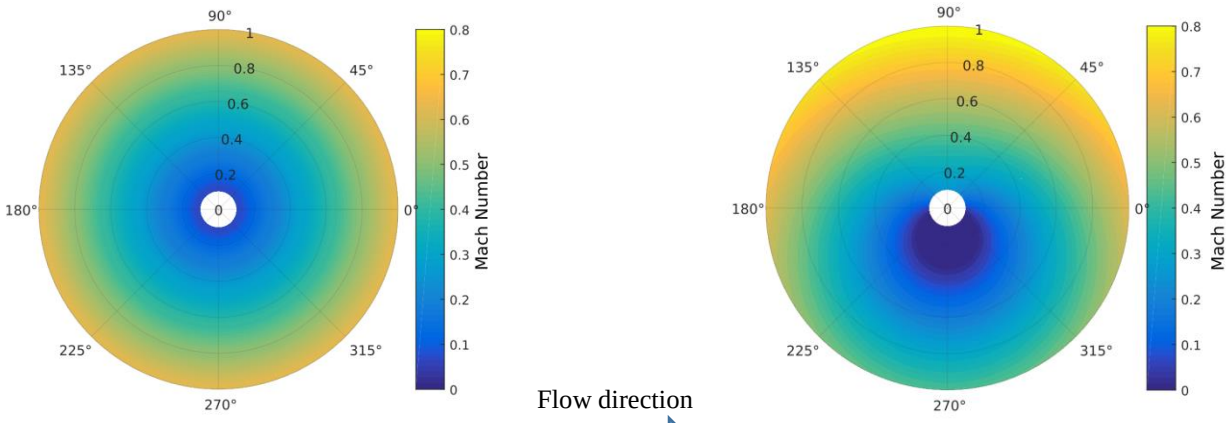

(a) Hover **(b) Forward flight – Advance ratio μ = 0.3**

Fig. 2 Mach number distribution over rotor disk for a tip speed of 218 m/s (ω = 44.4 rad/sec, R = 4.9m)

While looking at the requirements proposed by Campanile [5] and keeping in view the traditional aircraft structures, the question that remains open is whether the individual elements reflected in Fig. 3 optimize to the extent that a practical morphing solution is possible. Therefore, it is essential to extract as much flexibility as possible from

the given materials and/or structures without compromising strength and stiffness, and making conventional mechanisms as light as possible to reach an optimum design point. With this methodology, the optimal level of structural compliance is achievable, which is well suited to be adopted for a full-scale morphing implementation.

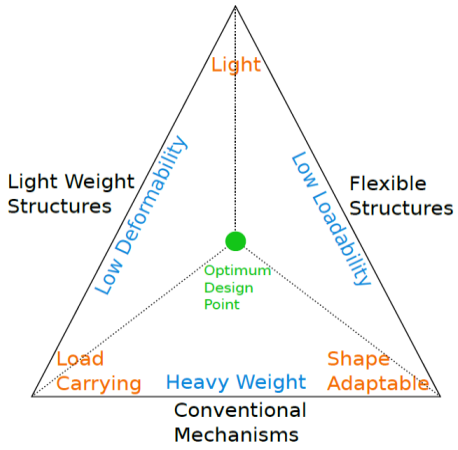

Fig. 3 Morphing requirement triangle [5].

In order to use existing structures in morphing perspective, Vos et al. [6] introduced the concept of introducing a discontinuity in the wing cross-section. This concept relied on introducing warping deformation of the wing skin, which was split at the trailing edge to create an open-section airfoil which has reduced torsional stiffness due to the cut, but which retains its original torsional stiffness when the cut is closed by an actuator. Later, Werter et al. [7] investigated an extension of this principle to the leading edge and trailing edge morphing devices mounted on a typical wingbox structure. This paper discusses the design process and implementation of the Translation Induced Camber (TRIC) concept for a blade of a rotorcraft and assess the potential advantages in terms of aerodynamic efficiency with respect to different morphing configurations and flight conditions. The research work is a part of European Union project SABRE (Shape Adaptive Blade for Rotorcraft Efficiency) under Horizon2020 (https://sabreproject.eu/).

The discussion in this paper is organized as follows. Section III describes the design requirements and objectives associated with the study. Section IV reviews the preliminary design in terms of methodology, CFD studies and actuators. Section V covers the outcomes of these studies and the results obtained against the objectives set in the earlier section. Section VI concludes the work.

III. Design Requirements

The design requirements laid down for the SABRE project are based on the Bo105 Helicopter and are stated in Table 1.

The preliminary design of the actuation system requires to achieve the following objectives.

1) Estimate the effects of materials and geometrical parameters on the actuation forces.
2) Determine the aerodynamic and inertial loading against which the actuator needs to operate.
3) Calculate the effectiveness of the resulting camber morphing in terms of aerodynamic coefficients and efficiency.
4) Given the volumetric and frequency constraints, select an appropriate actuator and design a mechanism around it.
5) Quantify the change in the critical mass and structural properties of original Bo105 blade as a result of modifications carried out for morphing.

Table 1 Design Requirements

Property	Unit	Value
Control method	-	Active camber
Rotor radius	m	4.91
Rotation speed	rad/sec	44.4
Blade chord	mm	270
Airfoil type	-	Bo105 (NACA 23012)
Mass per unit length	Kg/m	5.54
GJ	Nm^2	4850
EI flap	Nm^2	6820
EI lag	Nm^2	173000
EA	N	Not known
Flap deflection (downwards)	degree	8 (max)
Flap deflection (upwards)	degree	4 (max)
Frequency	-	Quasi-static to 2/rev or higher
Advance Ratio	-	0.3

IV. Preliminary Design

The operational principle of the TRIC concept shown in Fig. 4 is based on a hollow trailing edge portion (preferably made out of pre-preg composite material) while the rest of the blade is based on a conventional wing-box structure. This hollow trailing edge portion can be morphed as per the inputs to the actuation system. In case of an existing blade design as that of Bo105 considered in this work, this means that the main material characterization with respect to the original blade can remain the same. By introducing the required actuators and appropriate trailing edge changes, an effective morphing scheme can be implemented. In any case, this approach is very attractive in determining an optimum design while exploring the design variables in Fig. 3 because there are off-the-shelf materials and actuators that can be used for the morphing concept.

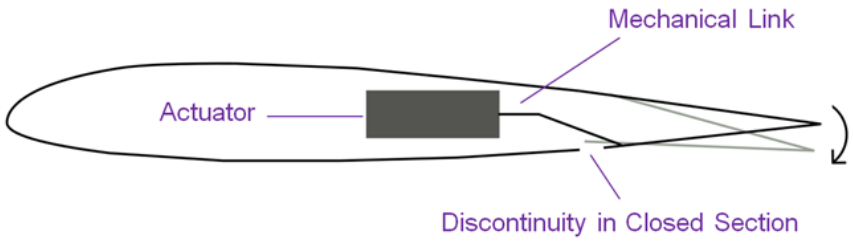

Fig. 4 TRIC concept

A. Methodology

The definition of a morphed configuration is shown in Fig. 5. Starting from the unmorphed or baseline configuration, the 2D flow analysis is carried out in ANSYS FLUENT to calculate the aerodynamic loads for various morphed configurations. These loads are then transferred to the Finite Element Analysis (FEA) software (ABAQUS) to determine the required actuator forces and obtain the morphed shapes under the influence of both elastic and aerodynamic loads. The boundary conditions employed in the FEA are depicted in Fig. 6. The top edge is fully constrained in all degrees of freedom while the two bottom edges are constraints in out of plane direction. The two nodes shown in Fig. 6 are subjected to displacement constraint in the chordwise direction giving the required morphed configuration. Consequently, the reaction forces for actuators are also estimated on these two nodes. A mesh convergence study is done for the analysis as shown in Table 2 on the basis of which a mesh size of 2 mm is chosen.

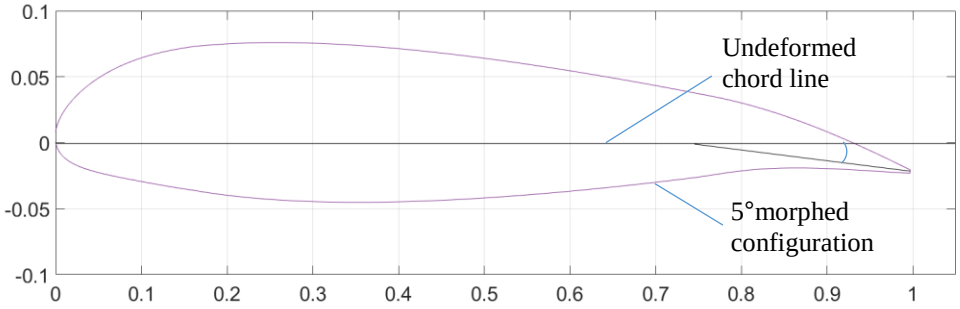

Fig. 5 Deflection angle definition

Table 2 Mesh Convergence Study

Mesh (mm)	Stress (MPa)	Reaction Force (N)
0.5	57.2	160
2	56	161
5	44	164

The resulting morphed shapes as shown in Fig. 7 are used for the subsequent analysis in Fluent to get the aerodynamic coefficients while the reaction forces obtained during these studies are used for actuator selection. Once the actuator selection is made based on the worst-case loads and centrifugal forces, the resulting information is employed in ABAQUS and CATIA for the detailed design and analysis.

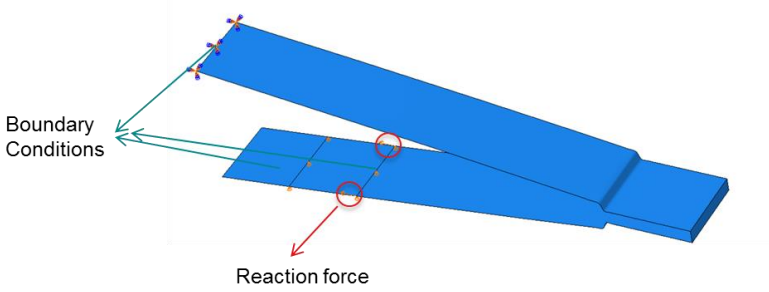

Fig. 6 Boundary conditions for TRIC concept

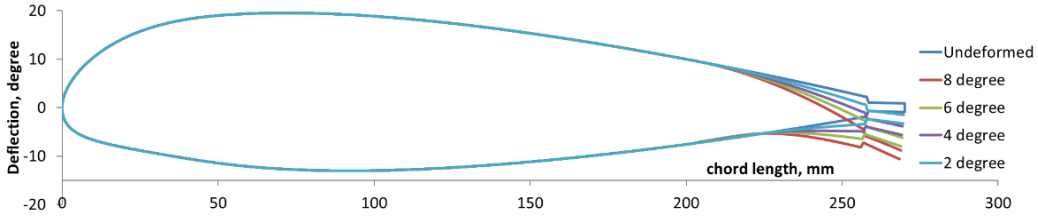

Fig. 7 Trailing edge camber morphing for different deflections.

The Fluid Structure Interaction (FSI) scheme employed in these studies is depicted in terms of a block diagram in Fig. 8, while the final output is shown in Fig. 9.

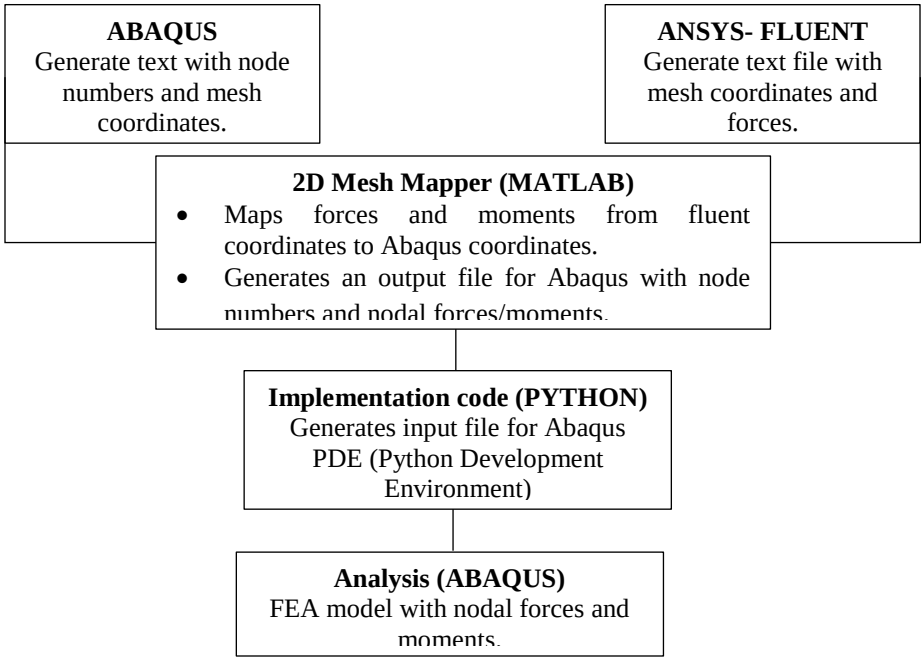

Fig. 8 Implementation of FSI scheme

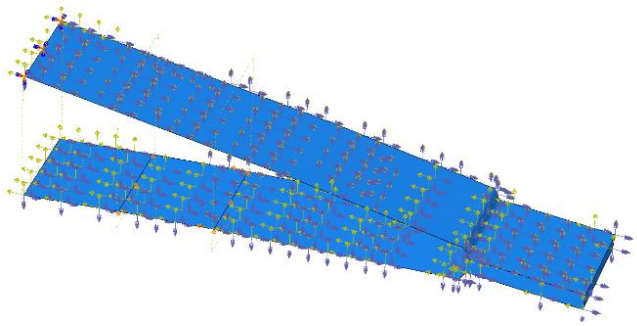

Fig. 9 Result of transfer of forces (green) and moments (blue) on a trailing edge segment

B. CFD Studies

In CFD simulations, the accuracy of the solutions are highly dependent upon on the quality of the mesh [8]. Numerous iterations are done using ICEM CFD to refine the mesh. The final refined mesh for the deformed and undeformed configurations is a C-grid mesh, as shown in Fig. 10. The airfoil shapes are placed in the center of this domain, and the airfoil surface is considered as a viscous wall. The dimensionless wall distance y+ is kept close to 1. The turbulence models used for the studies is the Spallart Allmaras (SA) model [15], which is a one-equation model.

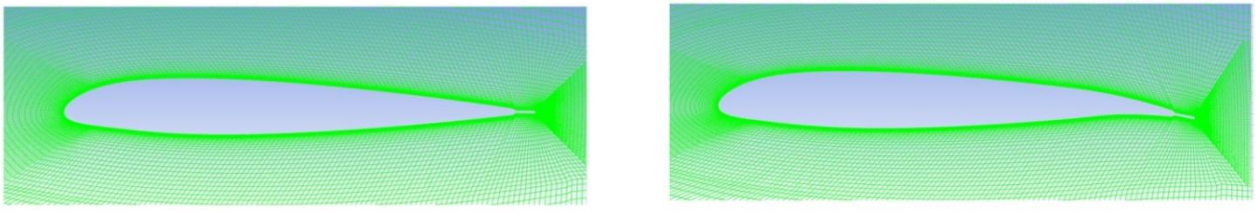

(a) Grid Mesh - Unmorphed case **(b) Grid Mesh - Morphed case**

Fig. 10 Grid mesh refinement

In order to validate the resulting mesh and settings, the results for the baseline configuration are compared to the experimental data [14] shown in Fig. 11, showing a good agreement between both the results.

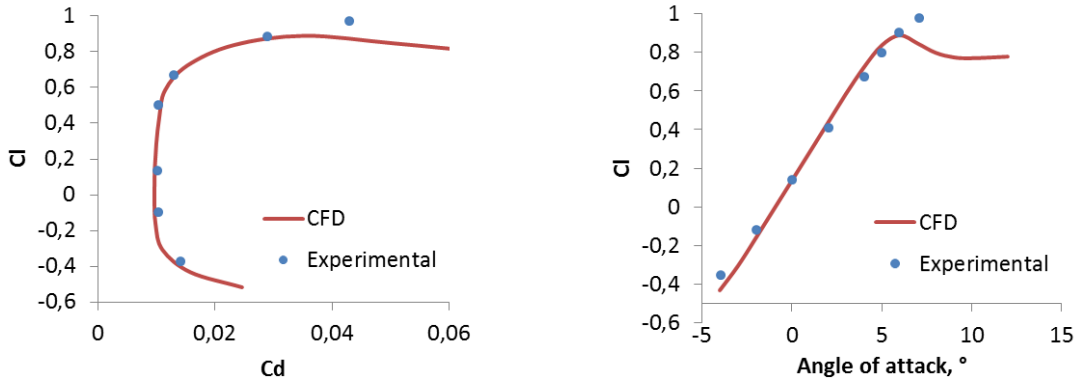

(a) Lift coefficient vs drag coefficient **(b) Lift coefficient as a function of angle of attack**

Fig. 11 Comparison of CFD and Experimental results for baseline configuration at Mach 0.6.

In order to determine the aeroelastic effects on the morphed shapes, deformations are observed at morphed configurations of 2°, 4°, 6° and 8° with respect to maximum and minimum loading conditions. The resulting shapes under the influence of both aerodynamic and elastic loads are plotted in Fig. 12 for a case of 2° deflection. It can be seen that the net displacements between the two sets of data points are minimum and hence, the aeroelastic effects may be neglected in such cases. A similar trend exists for other deformed configurations. Therefore, for all the subsequent CFD analyses, the deformed shapes for any particular configuration (0° to 8°) are kept fixed when analyzing for a particular Mach number and/or angle of attack in order to reduce the computational effort and time.

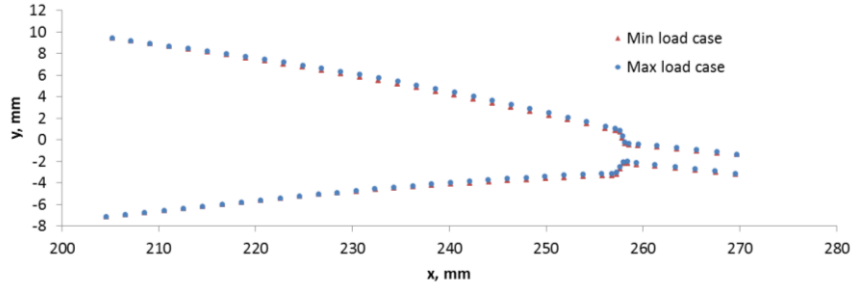

Fig. 12 Change in deformed shape as a result of maximum and maximum load cases.

C. Actuator Types

The type of actuator and its specifications are the key elements in the application of TRIC concept under the pre-set requirements. Given the volumetric constraint, three potential actuator options are investigated as shown in Fig. 13. Table 3 enlists the important advantages and disadvantages associated with each actuator type.

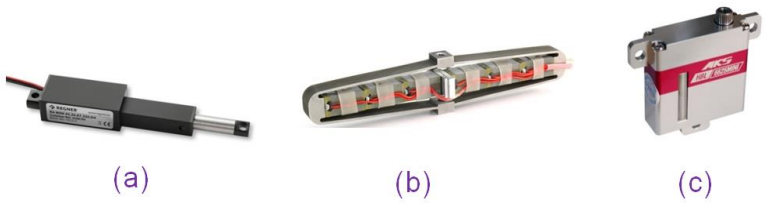

Fig. 13 Actuators considered (a) Linear actuators (b) Piezoelectric actuators (c) Servo drives

Table 3 Different types of actuators with Pros and Cons

Actuator Type	Pros	Cons
Linear Actuator	• Light weight. • Higher stroke lengths. • Relatively simple controls system. • Low-cost.	• Lower bandwidth. • Inherent delay in response. • Relatively lower force (more number of actuators required per unit length). • Use in a rotating environment not established.
Servo Motor	• Light weight. • Medium to high forces. • Low to medium operating frequency. • Relatively simple controls system. • Relatively inexpensive.	• Use in a rotating environment not established.
Piezoelectric (APA)	• Higher forces. • Higher operating frequencies. • References for its use in a rotating environment exist (Lee, et al., 2013), (Leconte & des Rochettes, 2002).	• Relatively heavy. • Limited stroke lengths. • Expensive

D. Centrifugal Loads

When a blade rotates, the flap experiences a centrifugal force which acts on a line through the center of rotation as shown in Fig. 14 and is given by

$$F = mr\omega^2 \tag{1}$$

For an initial estimate, the actuation mechanism is considered to be clamped to the main spar of the structure; hence the effect of the centrifugal force is estimated only for a flap of chordwise length equal to 24% of chord. The spanwise flap length is considered to be 1m, having a center located at 0.7R and skin thickness of 0.5mm carbon fibre prepreg material. In terms of total force required for the actuator, this component of centrifugal force accounts only to approximately 6% of the actuator force estimated for aerodynamic and elastic loads. This result indicates that in terms of forces, the actuator selection is mainly governed by the aerodynamic and elastic forces on the flap.

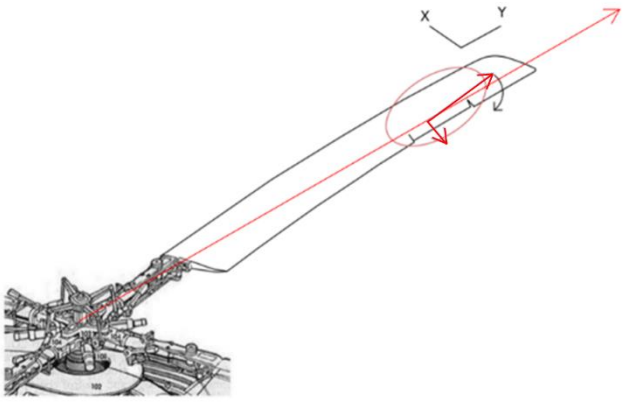

Fig. 14 Centrifugal force and its components on a rotor blade

V. Results

The results presented in this section are in line with the objectives defined in section III. These results are obtained for a trailing edge surface having a width of 10mm.

A. Effects of Material and Geometrical Parameters

For the skin of TRIC concept, prepreg composite material is used. Table 4 shows the effect of a few material options (mainly carbon fibre) and the resulting reaction force (under elastic loads only) for various layups for a 8° homogeneous deflection. The increase in skin thickness with current options increases the force considerably, hence, a skin thickness of 0.5 mm is considered suitable at this stage of design. Based on this study, AS4 with a quasi-isotropic layup and skin thickness of 0.5 mm is preferred.

Table 4 Effect of Material and Layup on Actuator Forces

Reaction Force (N)	Material	Skin Thickness (mm)	Layup
1.2	AS4	0.5	0/45/-45/90
0.874	AS4	0.5	0/0/45/90
0.358	AS4	0.5	0/0/0/0
1.2	T300	0.5	0/45/-45/90
1.8	T700	0.625	0/45/-45/90
0.86	Glass	0.5	0//90

The effect of the flap length is examined in order to finalize the morphed section. Studies are performed for a deflection from 6° to 8° for four different flap lengths, keeping the material, layup and thickness of the skin same. The RF (reaction forces) are computed for a flap width of 10mm and shown in Table 5.

Table 5 Actuator Forces for deflection

%Chord	RF due to Elastic loads (N)	RF due to combined loads (N)
20	1.26	4.32
22	1.2	4.68
24	0.79	5.0
25	0.69	6.0

The following observations are made during these studies.

I. The elastic forces tend to decrease if the flap length is increased. In contrast, the aerodynamic forces are increased by increasing the flap length.
II. Not considerably, but the actuator stroke (for a similar deflection) reduces when the flap length is decreased. This is important when considering the options of piezoelectric actuators which have inherently small stroke lengths.
III. The margin in the volume required for actuator connection/integration during assembly decreases by decreasing the flap length.

Based on these studies and keeping in view the potential actuator options, the flap length is taken as 24% of the chord length for the subsequent design and analysis.

B. Maximum Load Cases

The actuator used in the TRIC concept may encounter different magnitudes of forces during the flight operation. From a design perspective, it is important to consider the maximum or worst-case loads to determine the required actuation force. For this purpose, the load cases are computed for various Mach numbers and Angles of attack. A summary of maximum load cases is shown in Table 6. The maximum loading observed against a flap deflection of 6° to 8° is used for the actuator selection.

Table 6 Maximum load cases

TE rot (°)	Alpha (°)	Mach (-)	Cl (-)	Mach^2 x Cl (-)
0	3.7	0.7	0.651	0.318
2	2.5	0.7	0.762	0.373
4	1.5	0.7	0.857	0.420
6	1.5	0.7	0.988	0.484
8	1.5	0.7	1.068	0.523

C. Camber Morphing Effectiveness

Plots of lift and drag with respect to different angles of attack are presented in Fig. 15 showing that the lift coefficient increases with an increase in the morphing deflection up till around 14°.

In order to quantify the aerodynamic efficiency of the concept, the lift-to-drag ratio is plotted for different morphed configurations at Mach 0.185, as shown in Fig. 16. It can be seen that the ratio increases by increasing the trailing edge camber morphing. For $Cl \geq 1$ and higher deflection angles of 6° and 8°, this change in ratio is more pronounced and the highest value is obtained for a deflection of 6°. Similar plots for other Mach numbers can also be evaluated to determine precisely in which Mach regime, the highest efficiency is achieved [15]. This information is also helpful in determining the location of such a control surface over the entire length of the rotor blade.

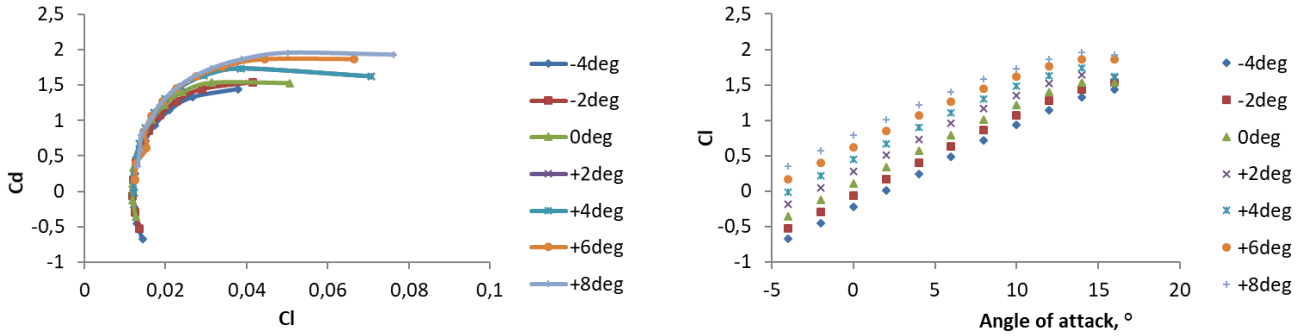

(a) Lift vs drag coefficient as a function of angle of attack **(b) Lift coefficient as a function of angle of attack**

Fig. 15 Plots of lift and drag coefficients at Mach 0.37 for different morphed configurations

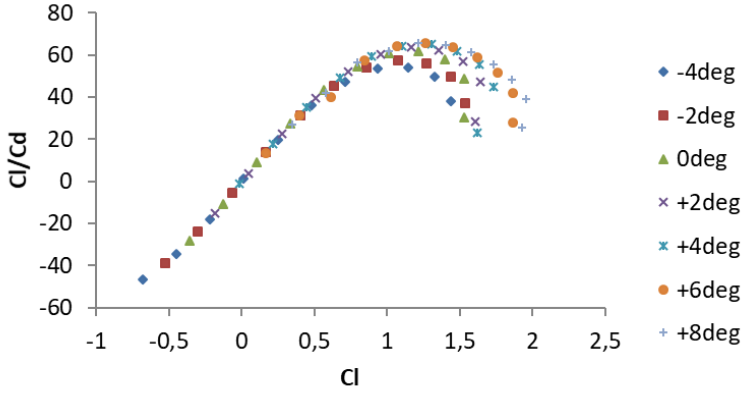

Fig. 16 Aerodynamic efficiency (cl/cd) as a function of lift coefficient

D. Actuator Selection

Amplified Piezoelectric Actuators (APA) manufactured by CEDRAT technologies [13] represent an attractive option for the rotorcraft application [11], [12]. Although the actuator strokes are limited, the higher force and frequency requirements are well covered by such actuators [13]. In fact, the operating frequencies of these actuators are sufficient to even fulfill the actuation requirements beyond 2/rev which are useful for noise and vibration mitigation. The limitation in stroke can be overcome by coupling the actuators in series enabling similar force with double the individual stroke length [13]. It must be noted that the servo drives, being less expensive and lightweight, also represent an attractive option. The main reason for disregarding servo drives in further mechanical design is the lack of evidence of its use under centrifugal loads. In contrast, the above referred piezoelectric actuators remain an appropriate choice keeping in view the required forces and frequencies in mind.

E. Change in Properties of the Existing Blade

It is important to know the amount of change in terms of critical structural parameters while incorporating the modifications in an existing blade like that of Bo105. Since the actual material characterization of Bo105 blade is not known, the material properties are extracted from the work of Kovalovs et al. [9] who used a similar geometric configuration in their research. After applying the boundary conditions, a unit load is applied in axial, flap-wise and lag-wise directions to calculate the corresponding deflections of the structure. Similarly, a unit moment is applied to calculate the twist. The representative CAD and FEA models are shown in Fig. 17.

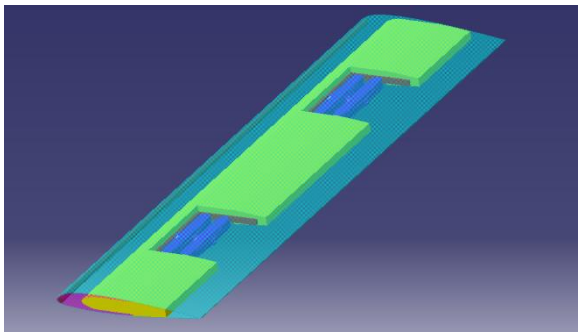

(a) Representative CAD model of blade section with modifications

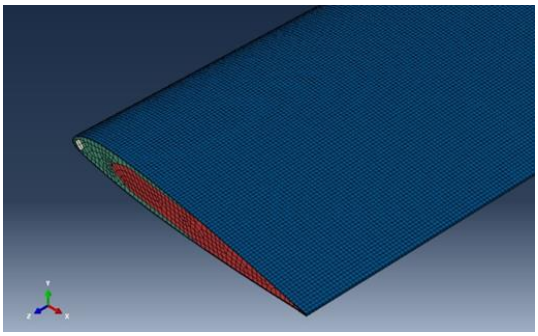

(b) FEA model of blade section

Fig. 17 Representative CAD and FEA models for preliminary estimations.

Using these deflections and twist in simple beam formulations [10], the required stiffness values are calculated for both the original and modified representative model of the Bo105 blade and listed in Table 7. Similarly, the changes in mass/meter and center of gravity are noted.

Table 7 Comparison of parameters for the original and modified representative models

Parameter	Original representative model (FEA)	Modified representative model	Percentage change
EI_1 (Nm2)	8230	8094.5	3.64%
EI_2 (Nm2)	167336	166417	1.65%
EA (N)	8.77e7	8.45e7	0.55%
GJ (Nm2)	3580	3195	10.75%
Mass/meter (kg/m)	5.545	6.336	14 %
X - C.G (m)	@ 24.6 % chord	@ 26.8 % chord	9%

Any modification in the existing blade design must not introduce an adverse dynamic response. Hence the parameters listed in Table 7 are evaluated to check whether the percentage change is significant or not. In this preliminary study, the percentage change is either close to 10% or well below, except for mass/meter change, which is 14%. These parameters are used for comprehensive analysis to assess the performance of the helicopter with morphing implementation and can be tuned during the iterative design process to the desirable levels.

VI. Conclusion

This work presents a preliminary design study of the Trailing Edge Induced Camber morphing concept for rotorcraft. For the baseline configuration, the blade of Bo105 is taken, and corresponding sizing and aerodynamic studies are performed accordingly. In addition, deformed shapes and required actuator forces are extracted for various aerodynamic load cases. Subsequently, the actuator selection is carried out considering the required forces, stroke, frequency, the complexity of the overall design, and available volume. Finally, some key parameters, which are required for comprehensive rotor analysis studies, are compared for the original and modified representative model of the Bo105 blade. The following conclusions are drawn at the end of this preliminary study.

1. Trailing edge camber morphing increases aerodynamic efficiency. For instance, referring to Fig. 16, the percentage increase in the maximum value of cl/cd (morphed vs. unmorphed configuration) turns out to be 6.5%.
2. The aeroelastic deformations can be accurately captured by the implementation of the FSI scheme that translates aerodynamic forces from CFD to Finite Element Analysis. In addition, it also enables actuator characterization.
3. The challenges in actuator selection for a rotor application increase due to volume constraints, centrifugal forces, and higher frequency requirements.
4. Piezoelectric actuators represent an attractive option for the actuation of control surfaces in rotorcraft due to their compact size, rigidity, and relatively higher frequencies. The limited stroke length can be negated to some extent by using amplified actuators such as those provided by CEDRAT technologies.
5. Implementing a trailing edge morphing solution with the piezo actuators increases the mass/meter of the blade by 14% while the C.G remains within 10%. Furthermore, the axial and bending stiffness changes are within 4%, while the torsional stiffness change is around 10%. These parameters can be used in comprehensive rotor analysis, and the design can be further refined based on the outcome of this analysis.

The future work involves building prototypes for wind tunnel tests at the University of Bristol, England, and whirl tower tests at the German Aerospace Center. These test campaigns are necessary for establishing a correlation between numerical modeling and corresponding test results.

Acknowledgments

This research work has received funding from the European Union's Horizon 2020 research and innovation program under grant agreement No. 723491.

References

[1] Peretz P. Friedmann and Thomas A. Millott. Vibration reduction in rotorcraft using active control- A comparison of various approaches. Journal of Guidance, Control, and Dynamics, 18(4):664-673,1995.
[2] Ephrahim Garcia. Smart structures and actuators: past, present, and future. (July 2002):1-12, 2002.
[3] Robert P Thornburgh, Andrew R Kreshock, Matthew L Wilbur, and Martin K Sekula. Continuous Trailing-Edge Flaps for Primary Flight Control of a Helicopter Main Rotor. AHS 70th Annual Forum, 2014.
[4] Silvestro Barbarino, Onur Bilgen, Rafic M. Ajaj, Michael I. Friswell, and Daniel J. Inman. A review of morphing aircraft. Journal of Intelligent Material Systems and Structures, 22(9):823-877, 2011.
[5] L. F. Campanile. Initial thoughts on weight penalty effects in shape-adaptable systems. Journal of Intelligent Material Systems and Structures, 16(1):47-56, 2005.
[6] R. Vos, Z. Gürdal and M. Abdalla, Mechanism for warp-controlled twist of a morphing wing, Journal of Aircraft, 47 (2) (2010) 450-457.
[7] Noud Werter, Jurij Sodja, Gregory Spirlet, and Roeland De Breuker. Design and Experiments of a Warp Induced Camber and Twist Morphing Leading and Trailing Edge Device. 24th AIAA/AHS Adaptive Structures Conference, (January):1-20, 2016.

[8] Farah Aqila, Mazharul Islam, Frenjo Juretic, Joel Guerrero, David H. Wood, Farid Nasir Ani. Study of Mesh Quality Improvement for CFD Analysis of an Airfoil. IIUM Engineering Journal, Vol. 19, No. 2, 2018.
[9] A. Kovalovs, E. Barkanov and S. Gluhihs. Active Twist of Model Rotor Blades with D-Spar Design. Journal of Transport, 2006.
[10] W. C. Young and R. G. Budynas. Roark's Formulas for Stress and Strain- Seventh Edition, McGraw-Hill.
[11] J. H. Lee, B. Natarajan, W. Jong Eu, V. S. R, J. Sang Park, T. Kim and S. Joon Shin. Structural and mechanism design of an active trailing-edge flap blade. Journal of Mechanical Science and Technology, 2013.
[12] P. Leconte and H. M. des Rochettes. Experimental Assessment of an Active Flap Device. American Helicopter Society 58th Annual Forum, Montréal, 2002.
[13] C. Technologies, Products Catalogue Version 5.1 - Cedrat Technologies actuator solutions.
[14] Dadone, L. U. US Army Helicopter Design Datcom Volume 1. Airfoils. No. D210-11097-1-Vol-1, Boeing VERTOL CO Philadelphia PA, 1976.
[15] Amine Abdelmoula and Jürgen Rauleder. Aerodynamic Performance of Morphed Camber Rotor Airfoils. AIAA Scitech 2019 Forum. 7-11 January 2019, San Diego, California.